Solar Energy 162 (2018) 489–499

Contents lists available at ScienceDirect

Solar Energy

journal homepage: www.elsevier.com/locate/solener

Feasibility study of seasonal solar thermal energy storage in domestic dwellings in the UK

Zhiwei Ma, Huashan Bao*, Anthony Paul Roskilly

Sir Joseph Swan Centre for Energy Research, Newcastle University, Newcastle-upon-Tyne NE1 7RU, UK

ARTICLE INFO

Keywords:
Seasonal solar thermal energy storage
Heating demand
Useful solar heat
Domestic dwelling

ABSTRACT

Seasonal solar thermal energy storage (SSTES) has been investigated widely to solve the mismatch between majority solar thermal energy in summer and majority heating demand in winter. To study the feasibility of SSTES in domestic dwellings in the UK, eight representative cities including Edinburgh, Newcastle, Belfast, Manchester, Birmingham, Cardiff, London and Plymouth have been selected in the present paper to study and compare the useful solar heat available on dwelling roofs and the heating demand of the dwellings. The heating demands of space and hot water in domestic dwellings with a range of overall heat loss coefficients (50 W/K, 150 W/K and 250 W/K) in different cities were calculated; then the useful heat obtained by the heat transfer fluid (HTF) flowing through tilted flat-plate solar collectors installed on the dwelling roof was calculated with varied HTF inlet temperature (30 °C, 40 °C and 50 °C). By comparing the available useful heat and heating demands, the critical solar collector area and storage capacity to meet 100% solar fraction have been obtained and discussed; the corresponding critical storage volume sizes using different storage technologies, including sensible heat water storage, latent heat storage and various thermochemical sorption cycles using different storage materials were estimated.

1. Introduction

Around 29% of energy in the United Kingdom in 2015 is consumed by the domestic sector, which represents the second largest proportion of final consumption, surpassing the industrial sector (Department for Business, Energy & Industrial Strategy, UK, 2016). The domestic sector is the most responsive to fluctuations in temperatures as about 80% of household final energy consumption is for space and water heating (Palmer and Cooper, 2013). The steadily growing number of household in the UK and the rising level of comfort requirement are the other two additional factors resulting in continuously increasing energy demand. In the meantime, gas and electricity prices have approximately doubled comparing to those in the year of 2002 (Palmer and Cooper, 2013). Upward pressures of household energy bill and imperative transition to a low carbon fuel supply for space and water heating stimulates the research and development of energy efficient technologies with higher penetration of renewable energy source, contributing to UK's ambitious target of decarbonised society with better living standard.

The total amount of solar radiation incident on the roof of a typical home exceeds its energy consumption over a year; however, the solar heating will require long-term heat storage to help balance differences between solar heat generation and demand requirements with respect to both disparities in time and magnitude (Pinel et al., 2011; Xu et al., 2014). Large scale seasonal solar thermal energy storage (SSTES) system using water as storage medium has been demonstrated in Germany (Mangold and Schmidt, 2009; Fisch et al., 1998) and Denmark (Fisch et al., 1998). These systems store solar heated hot water in tank, pit, borehole or aquifer layer for district heating system, and the storage volume is from hundreds cubic meter to more than ten thousands cubic meter. Small scale SSTES system for several or even individual residential dwelling is much less explored in practice, since the system volume required by seasonal storage based on conventional sensible heat storage method cannot be acceptably small. Chemical reaction, sorption and phase change material storage technologies have been proposed and developed to improve energy storage density, and have been applied to SSTES system (Pinel et al., 2011; Xu et al., 2014).

Solar thermal energy has not been extensively explored in the UK (Eames et al., 2014), and there is very limited information and studies on the feasibility and rationality of applying SSTES techniques for individual dwellings in the UK. Effort is required to seize the opportunity and promote solar thermal energy utilisation and SSTES application in the UK with particular consideration of different locations and climatic weather conditions. This paper conducted case studies to evaluate the potential and viability of SSTES application in individual dwellings in

* Corresponding author.
E-mail address: huashan.bao@newcastle.ac.uk (H. Bao).

https://doi.org/10.1016/j.solener.2018.01.013
Received 20 July 2017; Received in revised form 23 November 2017; Accepted 6 January 2018

Nomenclature

A	solar collector area (m^2)
c_p	specific heat (J/(kg K))
E	energy density (kWh/m^3)
I_h	global horizontal irradiance (kWh/m^2)
Q	heating load (kWh)
T	temperature (°C)
$\overline{UA}$	overall heat loss coefficient of dwelling (W/K)
$\dot{V}$	volumetric hot water consumption (m^3/h)
V	volume (m^3)

Greeks

β	slope of collector surface (°)
γ	surface azimuth angle (°)
ρ	density (kg/m^3)

Subscripts

a	ambient
cri	critical
CW	cold water
HD	heating demand
HW	hot water
i	inlet
R	room
sc	solar collector
SH	space heating
sto	storage
u	useful

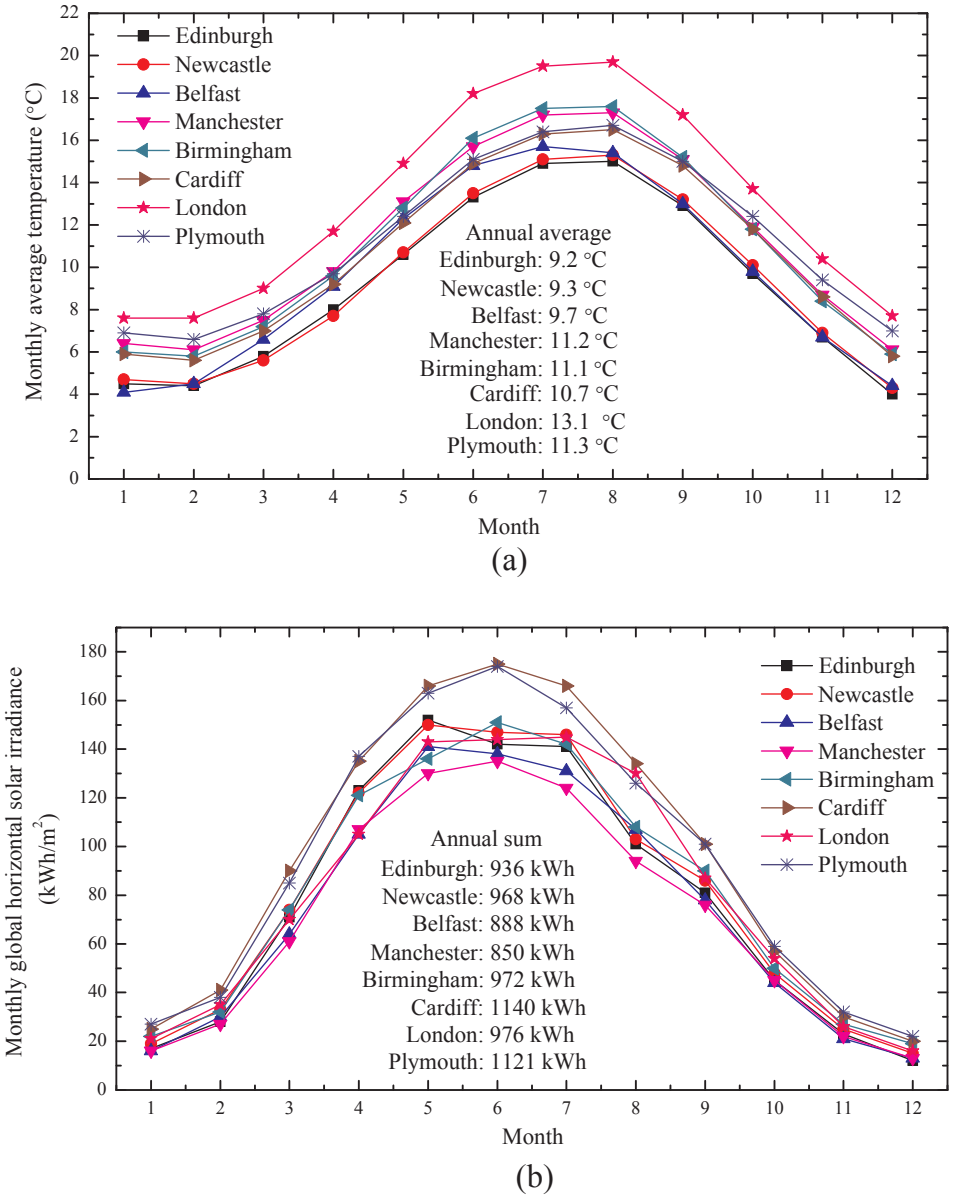

Fig. 1. Weather data of different cities, (a) monthly average temperature; (b) monthly global horizontal solar irradiance.

eight representative cities in the UK. The heating demands of dwellings and the useful solar heat potentially captured by flat-plate collector in each city were calculated and analysed. The critical values of solar collector area, storage capacity and the volume of heat storage system to achieve 100% solar fraction were calculated for dwellings with different overall heat loss coefficients.

2. Analysis method

2.1. Weather data

Hourly weather data including global horizontal radiation and ambient temperature of the selected eight cities, including Edinburgh, Newcastle, Belfast, Manchester, Birmingham, Cardiff, London and Plymouth from north to south, are available from the Meteonorm. Fig. 1 presents the monthly average ambient temperature T_a and the monthly total horizontal irradiance, I_h (kWh/m^2), representing the mean value between year 1991 and year 2010. As shown in the figure, the metropolis London has the highest ambient temperatures (annual average ambient temperature 13.1 °C) due to the urban heat island effect, while Edinburgh, Newcastle and Belfast have the lowest ambient temperature among all; Manchester has the lowest annual solar irradiance while Cardiff and Plymouth have the highest.

2.2. Useful solar thermal energy

The useful solar thermal energy gained by the heat transfer fluid (HTF) flowing through the used solar collector can be much less than the solar irradiance projected on the collector surface. This efficiency is dominated by the angle of incidence, the structure and the material of the collector itself and the heat loss to the atmosphere via conduction, convection and infrared radiation.

Flat-plate solar collector is used in the current study due to its mechanical simplicity and easy maintenance, and it is designed for application at moderate temperature level such as solar water heating, building heating and air conditioning. The method to determine the useful heat gained by the HTF flowing through a tilted flat-plate solar collector is given in Appendix A mainly adopted from literature (Duffie and Beckman, 2013). On the basis of weather data of global horizontal radiation and ambient temperature, the following steps were used in the calculation: (a) the available extraterrestrial solar irradiance was calculated based on time and collector location; (b) the beam and diffusion components were split by using sky clearness index; (c) the solar radiation on tilted surface was calculated; (d) finally, the useful heat was determined based on the geometry and material of the collector and more importantly on the inlet HTF temperature and heat loss coefficient.

As suggested by Eq. (A22) in Appendix A, the reduction from the absorbed solar irradiance to the useful heat collected by HTF depends on the collector heat removal factor, heat loss coefficient and HTF inlet temperature. The collector heat removal factor can be calculated based on the specification of the used collector as introduced in Appendix A, while the heat loss coefficient has been recommended by the collector manufacturer. In current study, different HTF inlet temperatures at 30 °C, 40 °C and 50 °C were studied to evaluate the useful heat.

2.3. Heating demand

2.3.1. Hot water

The UK domestic hot water consumption has been measured and the heating pattern has been identified in the work by Energy Saving Trust England (2008), where 68 regular and 39 combi boilers across the UK were monitored, the volumetric flow rate and the temperature of supplied hot water and feed cold water were recorded. The monthly variation of hot water volumetric consumption based on the whole sample and cold water feed temperature at different regions are presented in Table 1. The lowest monthly hot water consumption occurs in April and July which was contributed to the Easter and summer holidays. The percentage of water consumption in each hour through a day was estimated on the basis of whole measured sample as shown in Fig. 2. Therefore the hourly hot water consumption (m^3/h) throughout a whole year can be estimated; accordingly, the hourly hot water heating demand, Q_{HW} (kWh), can be calculated by the following equation:

$$Q_{HW} = c_p \rho_{HW} \dot{V}_{HW} (T_{HW} - T_{CW})/1000 \quad (1)$$

where c_p is the average specific heat of inlet cold water and supply hot water (J/(kg K)), $\dot{V}_{HW}$ is the hourly volumetric hot water consumption (m^3/h), ρ_{HW} is the hot water density. The hot water temperature T_{HW} can be considered at a constant value of 52 °C according to literature (Energy Saving Trust England, 2008), while the inlet cold water temperature T_{CW} is varied with time and location as given in Table 1.

2.3.2. Space heating demand

In current study a simple method of calculating the space heating demand, Q_{SH} (kWh) as given in Eq. (2) was used, which attributed the heat loss to the temperature difference between the inside and outside of a dwelling and a parameter named overall heat loss coefficient (Karacavus and Can, 2009):

$$Q_{SH} = \overline{UA}(T_R - T_a)/1000 \quad (2)$$

where $\overline{UA}$ is the overall heat loss coefficient (W/K) of the whole dwelling, T_R is the room temperature and T_a is the ambient temperature. The $\overline{UA}$ value depends on dwelling floor area, the insulation condition and the external wind speed, and it has been measured and reported varying from approximately 50 W/K to 300 W/K for the UK dwellings (Johnston et al., 2010; Stafford et al., 2012; Johnston and Siddall, 2016). Therefore, three $\overline{UA}$ values, 50 W/K, 150 W/K and 250 W/K were used in current calculation to exemplify three different levels of dwelling heat losses. The average indoor temperature when the heating system is switched on is in a narrow range of 20.5–21.5 °C in the UK (Kane et al., 2015), hence T_R was given at 21.0 °C in current study.

2.4. Calculation framework and system sizing

The present calculation followed the framework shown in Fig. 3. After obtaining the heating demand and useful heat, the critical solar collector area $A_{sc,cri}$ to satisfy all the heating demand can be calculated by Eq. (3).

Table 1
Hot water consumption and cold water temperature in different month.

Month	Mean hot water consumption (L/day)	Cold water temperature (°C)			
		South England[a]	Midlands[b]	North England[c]	Scotland[d]
Jan	116.86	12.06	12.94	9.62	9.62
Feb	124.64	11.33	13.31	9.32	9.15
Mar	125.71	12.39	14.32	10.70	9.68
Apr	114.74	15.28	16.30	13.70	13.27
May	122.88	16.14	17.68	15.32	14.49
Jun	116.50	19.33	19.72	17.26	16.76
Jul	98.44	21.17	21.73	19.33	19.49
Aug	105.52	20.09	20.12	18.67	18.44
Sep	112.61	19.56	20.31	17.88	17.52
Oct	123.58	16.80	17.81	15.55	15.05
Nov	127.84	13.70	15.31	12.22	13.73
Dec	133.16	12.39	14.03	10.51	12.39
Average	118.54	15.85	16.97	14.17	14.13

[a] Cardiff, London and Plymouth.
[b] Manchester and Birmingham.
[c] Newcastle and Belfast.
[d] Edinburgh.

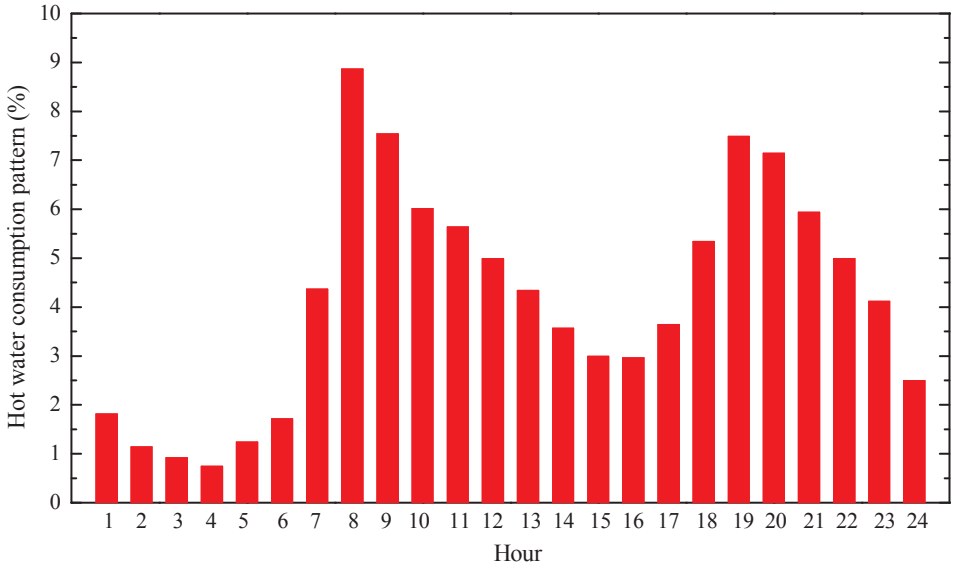

Fig. 2. Hourly hot water consumption pattern in the UK (Energy Saving Trust England, 2008).

$$A_{sc,cri} = \frac{\sum Q_{HD}}{\sum Q_u} \quad (3)$$

where ΣQ_{HD} is the annual total heating demand, ΣQ_u is the annual total useful heat captured by one square meter collector. Then the critical storage capacity, $Q_{sto,cri}$ can be calculated as the excess useful heat captured after meeting the heating demand, as given in the following equation.

$$Q_{sto,cri} = \sum (Q_u * A_{sc,cri} - Q_{HD})_{Q_u * A_{sc,cri} > Q_{HD}} \quad (4)$$

The storage volume can be calculated by Eq. (5) based on the storage energy density, E, of the used storage technology.

$$V_{sto,cri} = \frac{Q_{sto,cri}}{E} \quad (5)$$

3. Results and discussion

3.1. Heating demand

On the basis of method introduced in Section 2.3, the hourly, daily, monthly and annual heating demands of hot water and space heating in eight representative UK cities can be obtained. The annual heating demands are listed in Table 2, where the overall heat loss coefficient of the dwelling is exemplified as 50 W/K, 150 W/K and 250 W/K. The heating demand for hot water is dominated by the cold water feed temperature since the delivered hot water temperature was considered as constant; therefore Manchester and Birmingham have the lowest hot water heating demand due to their relatively higher cold water temperature.

According to Eq. (2), the heating demand for space heating is the function of ambient temperature if $\overline{UA}$ is at a constant value. That

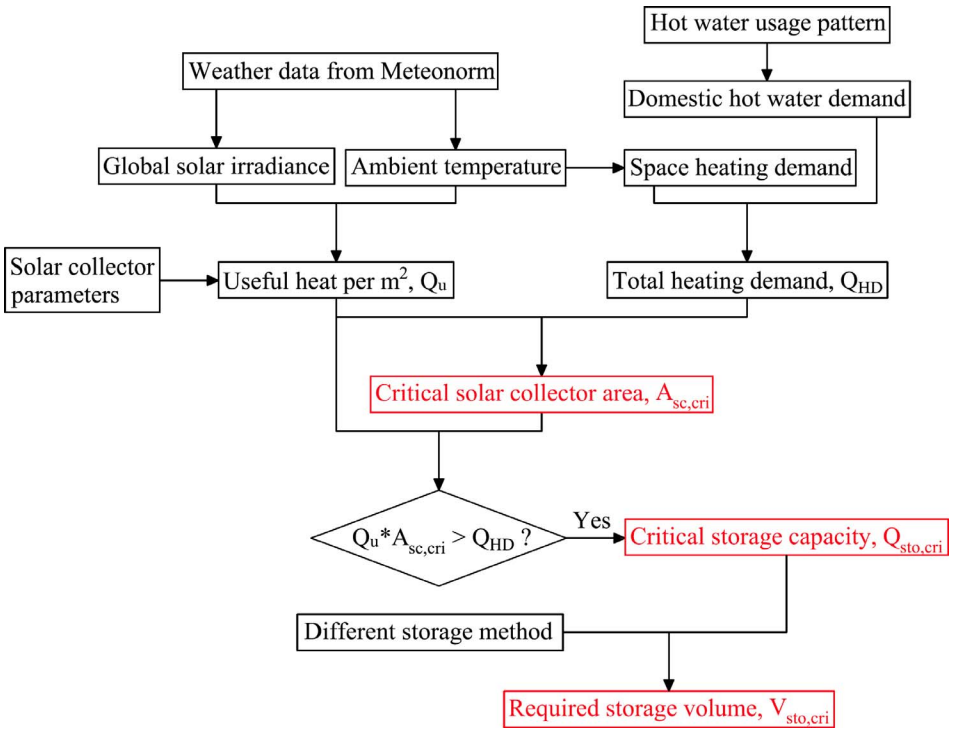

Fig. 3. Calculation framework of current study.

Table 2
Annual heating demands in different cities in the UK.

	Q_{HW} (kWh)	$Q_{HD} = Q_{HW} + Q_{SH}$ (kWh)		
		$\overline{UA}$ = 50 W/K	$\overline{UA}$ = 150 W/K	$\overline{UA}$ = 250 W/K
Edinburgh	1887.33	7095.87	17512.85	27929.91
Newcastle	1886.44	7025.97	17304.99	27584.56
Belfast	1886.44	6856.01	16795.04	26734.68
Manchester	1745.78	6067.45	14710.79	23354.13
Birmingham	1745.78	6114.65	14852.39	23590.13
Cardiff	1802.85	6334.16	15396.68	24459.71
London	1802.85	5370.60	12506.03	19641.46
Plymouth	1802.85	6082.89	14642.91	23202.94

implies London, Plymouth and Manchester have the lowest space heating demands due to their relatively higher ambient temperature. Apparently, larger value of $\overline{UA}$, which could be caused by larger floor area or poorer insulation, leads to larger heating demand. With a low overall heat loss coefficient, e.g. 50 W/K, the heat demand for space heating could be only 3–4 times as large as that for hot water; this ratio could be about 13–14 for a dwelling having 250 W/K overall heat loss coefficient.

3.2. Useful solar thermal energy

The solar collector slopes (β) of 30°, 45° and 60° have been analysed, and the results showed that the collector with $\beta = 45°$ yielded the largest annual useful heat amount in all studied cities, hence the further evaluation was carried out using 45° collector slope. Moreover, the solar collector facing due south, i.e. the collector azimuth angle $\gamma = 0$, was assumed to ensure the maximum solar heat capture.

The monthly useful heat obtained by HTF with different inlet temperature are shown in Fig. 4 in the comparison with monthly heating demands, where the solar collector area is exemplified at 20 m^2. Lower HTF inlet temperature implies smaller temperature difference between the fluid and the ambient, leading to less heat loss to the ambient, therefore more useful heat can be expected as shown in the figure; however, the obtained useful heat has lower quality in this case. For a dwelling with 50 W/K overall heat loss coefficient, 20 m^2 solar collector is almost enough to cover all the heating demand overall a year with 30 °C and 40 °C HTF inlet temperature; however, for dwelling with larger floor area or poorer insulation, 20 m^2 solar collector can hardly meet the heating demand even in the summer in cold cities like Edinburgh, Newcastle and Belfast.

3.3. Critical solar collector area and storage capacity

Critical solar collector area and the corresponding storage capacity required are defined as the situation when the heating demand of the targeted dwelling is 100% fully provided by solar thermal energy with seasonal storage (100% solar fraction).

Table 3 gives both of the critical solar collector area and storage capacity in the case of 50 W/K, 150 W/K and 250 W/K overall heat loss coefficient and 30 °C, 40 °C and 50 °C HTF inlet temperature. As can be seen from the table, the critical solar collector areas are in range of 10.76–31.60 m^2, 25.79–77.41 m^2 and 40.51–123.22 m^2 in the case of 50 W/K, 150 W/K and 250 W/K overall heat loss coefficient respectively, while the corresponding ranges of critical storage capacity are 2331.91–3235.26 kWh, 5821.50–8189.00 kWh and 9311.10–13143.01 kWh. These storage capacities account for about 38.2–52.6% of the total heating demands.

The domestic houses in the UK with two to five bedrooms have a mean floor area of 69.2–158.7 m^2 (Wilson, 2010), therefore the available roof area to install solar collector is estimated between 24.46 m^2 and 56.1 m^2 considering two storey and 45° pitched roof. In this case, the roof area cannot meet the requirement of 100% solar fraction with SSTES system if the overall heat loss coefficient is large, e.g. 250 W/K or the HTF inlet temperature is high, e.g. 50 °C, as can be seen from Table 3.

As the increase of HTF inlet temperature from 30 °C to 50 °C, the critical solar collector area must be enlarged to cope with the increasing heat loss, this enlargement is in the range of 67–83% as being calculated in all study cases; meanwhile the critical storage capacity changes only 5.1–9.3%. These two critical values will become almost four times larger as the overall heat loss coefficient increasing from 50 W/K to 250 W/K since the heating demand increases at the same ratio.

Belfast has the poorest condition for SSTES since that its solar radiation and average ambient temperature are both low, which leads to the largest critical solar collector area and storage capacity; Manchester takes the second position of least suitable for SSTES application due to its lowest solar radiation in despite of its high ambient temperature. The south cities Cardiff, London and Plymouth have the most preferable condition to apply SSTES. Cardiff enjoys the lowest critical solar collector area due to the smallest difference between heating demand and useful heat, while Plymouth requires the lowest critical storage capacity because of its lowest temperature difference between summer and winter.

3.4. Critical storage volume

The critical storage volume to satisfy 100% solar fraction using different thermal energy storage technologies can be estimated based on the energy densities given by literature (Hadorn, 2008), which estimated the storage volumes required for a storage capacity of 1850 kWh with 25% heat loss were 1 m^3, 10 m^3, 20 m^3 and 34 m^3 respectively for chemical reaction storage, sorption storage, phase change material storage and water sensible heat storage.

Take the moderate overall heat loss coefficient at 150 W/K as an example, the critical storage volume using sorption storage is 31.5–44.3 m^3 in all studied cities. Critical values of using other storage technologies can be proportionally calculated according to the data provided by literature (Hadorn, 2008), for example, if using water as the storage material, this storage volume should be in the range of 107.1–150.62 m^3. Nevertheless, in reality, the energy density of SSTES system depends on the system structure and scale, some experimentally tested energy densities of SSTES prototype and corresponding critical storage volume are shown in Fig. 5.

Current results are based on the situation of 100% solar fraction for domestic heating with 21 °C room temperature all through a year, which might not be practical; however, these results can be used as baselines or fundamental database, then the SSTES system performance with lower solar fraction or shorter space heating period can be reasonably estimated.

4. Conclusions

To study the feasibility of applying seasonal solar thermal energy storage in domestic dwellings in the UK, the heating demands for space heating and hot water and the useful solar heat available in eight UK cities were calculated and compared. The critical solar collector area, storage capacity and storage volume of different storage systems to fully cover the heating demands using solar heat throughout a year have been calculated and compared. The primary findings are made as follows.

(a) The annual heating demands of all studied cities were in the range of 5370.6–7095.9 kWh, 12506.0–17512.9 kWh and 19641.5–27929.9 kWh when the overall heat loss coefficient of the dwelling was 50 W/K, 150 W/K and 250 W/K respectively.

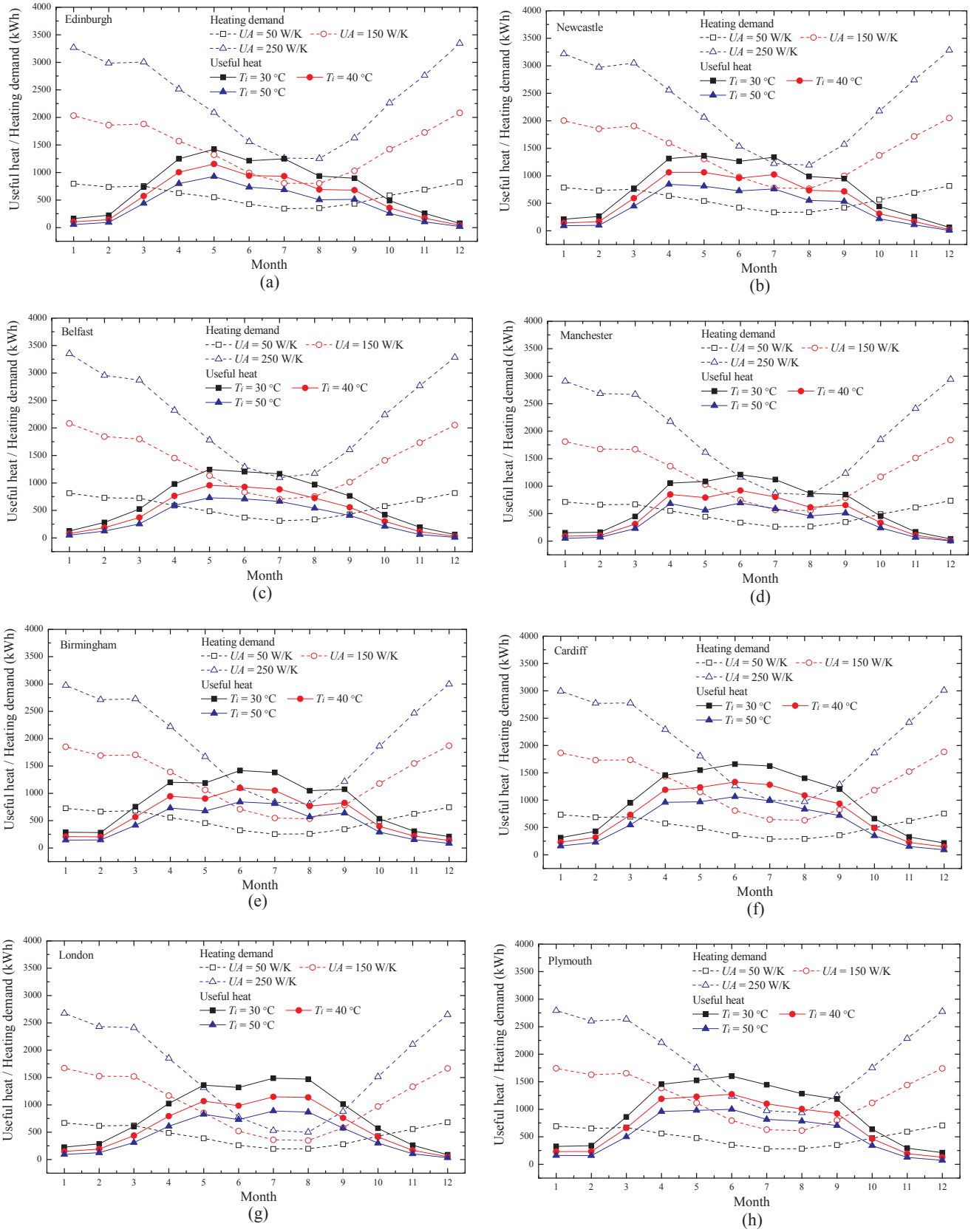

Fig. 4. Monthly heating demands and useful heat in different cities in the UK, A_{sc} = 20 m^2, β = 45°, γ = 0°.

Table 3
Critical solar collector area and storage capacity, $\beta = 45^{\circ}$, $\gamma = 0^{\circ}$.

	$\overline{UA}$ (W/K)	T_i = 30 °C		T_i = 40 °C		T_i = 50 °C	
		$A_{sc,cri}$ (m^2)	$Q_{sto,cri}$ (kWh)	$A_{sc,cri}$ (m^2)	$Q_{sto,cri}$ (kWh)	$A_{sc,cri}$ (m^2)	$Q_{sto,cri}$ (kWh)
Edinburgh	50	15.94	2821.82	20.91	2920.94	27.69	3032.61
	150	39.35	7177.55	51.61	7422.17	68.35	7697.79
	250	62.75	11533.40	82.30	11923.54	109.00	12363.10
Newcastle	50	15.26	2814.75	20.21	2925.75	27.04	3031.57
	150	37.60	7135.07	49.78	7408.47	66.61	7669.11
	250	59.93	11455.53	79.35	11891.34	106.18	12306.81
Belfast	50	17.30	2959.15	23.30	3093.35	31.60	3235.26
	150	42.38	7512.62	57.09	7841.37	77.41	8189.00
	250	67.46	12066.34	90.87	12589.65	123.22	13143.01
Manchester	50	15.99	2744.52	21.76	2842.32	29.31	2919.09
	150	38.76	6928.86	52.76	7165.98	71.07	7352.11
	250	61.54	11113.19	83.77	11489.63	112.82	11785.13
Birmingham	50	12.64	2432.60	16.72	2485.02	22.26	2563.21
	150	30.71	6198.41	40.62	6325.74	54.08	6515.66
	250	48.78	9964.21	64.51	10166.45	85.89	10468.11
Cardiff	50	10.76	2426.40	13.79	2511.01	17.95	2614.28
	150	26.14	6130.69	33.51	6336.35	43.63	6587.36
	250	41.53	9835.19	53.23	10161.90	69.31	10560.68
London	50	11.08	2448.27	14.72	2535.12	19.69	2624.96
	150	25.79	6065.04	34.29	6267.29	45.86	6476.50
	250	40.51	9681.82	53.85	9999.46	72.02	10328.03
Plymouth	50	10.91	2331.91	14.11	2436.48	18.47	2534.49
	150	26.25	5821.50	33.98	6073.25	44.45	6309.16
	250	41.60	9311.10	53.84	9710.01	70.44	10083.83

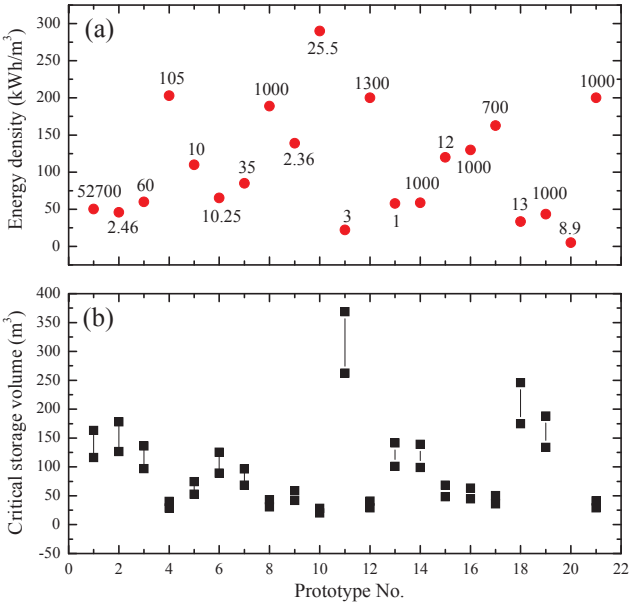

Fig. 5. (a) Energy densities of SSTES prototypes, the number besides the dot symbol is the prototype system scale in unit of kWh; (b) corresponding critical storage volumes. $\beta = 45^{\circ}$, $\gamma = 0^{\circ}$, $\overline{UA}$ = 150 W/K. Storage technology: 1. Hot water in pebble-bed storage (Hahne, 2000); 2. $Na_2HPO_4{\cdot}12H_2O$ supercooling latent heat storage (Hirano and Saitoh, 2007); 3. Closed $SrBr_2$-water sorption (Mauran et al., 2008); 4. Open $SrBr_2$-water sorption (Michel et al., 2014); 5. Closed LiBr-water sorption (Zhang et al., 2014); 6–8: Closed LiCl-water sorption (Zhao et al., 2016; Bales, 2008); 9: Open $MgCl_2$-water sorption (Zondag et al., 2013); 10: Open vermiculite-$CaCl_2$-water sorption (Aydin et al., 2016); 11–14: Closed zeolite-water sorption (Bales, 2008; Finck et al., 2014; Hauer, 2002); 15–17: Open zeolite-water sorption (Bales, 2008; Weber et al., 2016); 18–19: Closed silica gel-water sorption (Bales, 2008); 20–21: Closed NaOH-water sorption (Bales, 2008).

(b) The increase of HTF inlet temperature from 30 °C to 50 °C to pursue high quality heat led to 67–83% and 5.1–9.3% increase on the critical solar collector area and storage capacity.
(c) The critical storage volume was in the range of 31.5–44.3 m^3 if using sorption storage method with 150 W/K overall heat loss coefficient; while storage volumes using other storage materials can be proportionally calculated.
(d) Belfast was found to have the poorest condition to implement SSTES, at the moderate conditions of 150 W/K overall heat loss coefficient and 40 °C HTF inlet temperature, the critical solar collector area and storage capacity were 57.09 m^2 and 7841.37 kWh respectively. In this case, the required solar collector area was larger than the average available roof area of detached house in the UK.
(e) Cardiff, London and Plymouth have the greater potential to develop SSTES domestic application, the critical solar collector area and storage capacity were 33.51–34.29 m^2 and 6073.25–6336.35 kWh respectively in the case of 150 W/K overall heat loss coefficient and 40 °C HTF inlet temperature.

Acknowledgement

The authors gratefully acknowledge the support from the Heat-STRESS project (EP/N02155X/1) funded by the Engineering and Physical Science Research Council. Data supporting this publication is openly available under an 'Open Data Commons Open DatabaseLicense'. Additional metadata are available at: https://doi.org/10.17634/152536-4. Please contact Newcastle Research Data Service at rdm@ncl.ac.uk for access instructions.

Appendix A

Determination of available useful solar heat based on pyranometer data (Duffie and Beckman, 2013).

A.1. Available extraterrestrial solar irradiance

The extraterrestrial radiation, G_{on}, incident on the surface normal to the radiation is dependent on the time through a year and can be calculated by the following equation.

$$G_{on} = G_{sc}\left(1 + 0.033\cos\frac{360n}{365}\right) \tag{A1}$$

where G_{sc} is the solar constant, which is 1367 W/m^2; n is the number of the day through a year.

To calculate the extraterrestrial radiation incident on a surface, the angle of incidence, θ, between the beam radiation and the normal to the surface should be known. Fig. A1 is given to assist the calculation of θ, and the following equation is used.

$$\cos\theta = \sin\delta\sin\phi\cos\beta - \sin\delta\cos\phi\sin\beta\cos\gamma + \cos\delta\cos\phi\cos\beta\cos\omega + \cos\delta\sin\phi\sin\beta\cos\gamma\cos\omega + \cos\delta\sin\beta\sin\gamma\sin\omega \tag{A2}$$

where ϕ is the latitude of the location of the collector surface, northern hemisphere positive and southern hemisphere negative; β is the slope of the surface; γ is the surface azimuth angle, which is zero due south and east negative, west positive; ω is the hour angle, 15° per hour, morning negative, afternoon positive; δ is the declination of the sun which can be calculated by the following equation.

$$\delta = \frac{180}{\pi}(0.006918 - 0.399912\cos B + 0.070257\sin B - 0.006758\cos 2B + 0.000907\sin 2B - 0.002697\cos 3B + 0.00148\sin 3B) \tag{A3}$$

where $B = 360(n-1)/365$.

For a horizontal surface, $\beta = 0$, $\theta = \theta_z$, Eq. (A2) can be simplified as

$$\cos\theta = \cos\theta_z = \sin\delta\sin\phi + \cos\delta\cos\phi\cos\omega \tag{A4}$$

Therefore, the extraterrestrial solar irradiance on a horizontal surface can be calculated based on the following equation as illustrated by Fig. A2.

$$G_{oH} = G_{on}\cos\theta_z = G_{sc}\left(1 + 0.033\cos\frac{360n}{365}\right)\cos\theta_z \tag{A5}$$

At any interval from ω_1 to ω_2, the extraterrestrial solar irradiance on a horizontal surface can be obtained by integrating Eq. (A5).

$$I_{oH} = \frac{12\times 3600}{\pi}G_{sc}\left(1 + 0.033\cos\frac{360n}{365}\right)\left[\cos\phi\cos\delta(\sin\omega_2 - \sin\omega_1) + \frac{\pi(\omega_2-\omega_1)}{180}\sin\phi\sin\delta\right] \tag{A6}$$

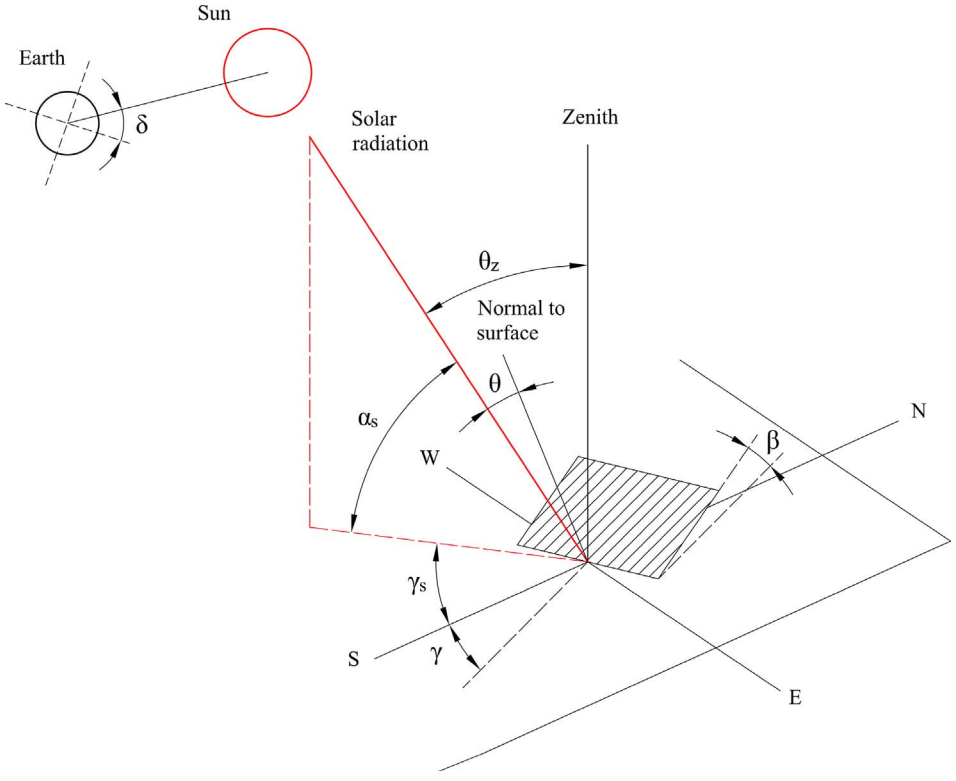

Fig. A1. Angles related to solar beam radiation.

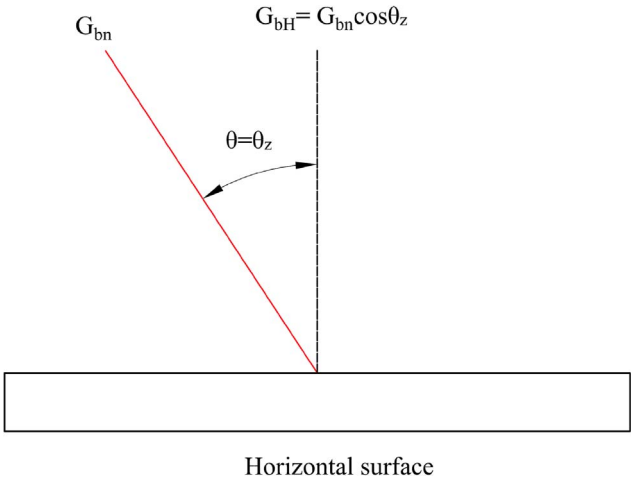

Fig. A2. Solar beam radiation on a horizontal surface.

A.2. Beam and diffusion components

The solar radiation measured by a horizontal pyranometer consists of beam and diffusion. The fractions of these two components can be estimated based on the hourly clearness index, k_T,

$$k_T = \frac{I_H}{I_{oH}} \tag{A7}$$

where I_H is the hourly solar irradiance measured on a horizontal surface, commonly available as pyranometer measurement data. Then the diffusion fraction can be calculated by the following c.

$$\frac{I_{dH}}{I_H} = \begin{cases} 1.0-0.09k_T & \text{for } k_T \leqslant 0.22 \\ 0.9511-0.1604k_T + 4.388k_T^2-16.638k_T^3 + 12.336k_T^4 & \text{for } 0.22 < k_T \leqslant 0.80 \\ 0.165 & \text{for } k_T > 0.80 \end{cases} \tag{A8}$$

I_{dH} is the hourly diffusional irradiance on a horizontal surface. Then the beam radiation I_{bH} can be calculated as $I_{bH} = I_H - I_{dH}$.

A.3. Solar radiation on tilted surface

Based on the measured hourly horizontal solar irradiance I_H and its component I_{bH} and I_{dH}, the solar radiation on a titled surface, I_T can be determined by the following equations.

$$I_T = I_{bH}R_b + I_{dH}\left(\frac{1+\cos\beta}{2}\right) + I_H\rho_g\left(\frac{1-\cos\beta}{2}\right) \tag{A9}$$

$$R_b = \frac{G_{bT}}{G_{bH}} = \frac{\cos\theta}{\cos\theta_z} \tag{A10}$$

where ρ_g is the reflectance of the ground; θ and θ_z should be in the range of 0 to 90°.

A.4. Solar thermal energy absorbed by flat-plate solar collector

The solar thermal energy incident on a collector is not 100% absorbed by the absorber due to the transmission, reflection and absorption by different parts of the solar collector. As shown in Fig. A3, a transmittance-absorptance product, $\overline{\tau\alpha}$, is calculated as the ratio of the absorbed

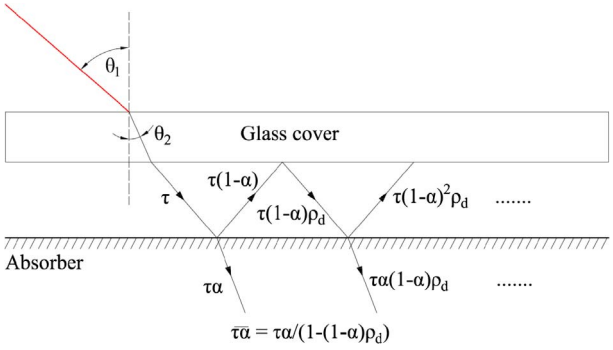

Fig. A3. Solar radiation absorption by an absorber covered by glass.

radiation to the total incident radiation by the following equation.

$$\overline{\tau\alpha} = \frac{\tau\alpha}{1-(1-\alpha)\rho_d} \cong 1.01\tau\alpha \tag{A11}$$

where τ is the transmittance of the glass cover and α is the absorptance of the absorber plate, both of which are the function of incident angle; ρ_d is the reflectance of the glass cover.

The transmittance of the glass cover is approximately the product of absorption transmittance τ_a and reflection transmittance τ_r

$$\tau \cong \tau_a \tau_r \tag{A12}$$

The equation of the absorption transmittance is

$$\tau_a = \exp\left(-\frac{KL}{\cos\theta_2}\right) \tag{A13}$$

where K is the extinction coefficient, varying form about 4–32 m^{-1} dependent on different type glass. L is the thickness of the glass cover. θ_2 is the incident angle to the absorber plate, as shown in Fig. A3, and the following equation is used to determine θ_2.

$$n_1 \sin\theta_1 = n_2 \sin\theta_2 \tag{A14}$$

n is the refraction index, glass has an average value of 1.526 while air has a value near 1.

The following equations can be used to determine the reflection transmittance.

$$\tau_r = \frac{1}{2}\left(\frac{1-r_\parallel}{1+r_\parallel} + \frac{1-r_\perp}{1+r_\perp}\right) \tag{A15}$$

$$r_\parallel = \frac{\sin^2(\theta_2-\theta_1)}{\sin^2(\theta_2+\theta_1)} \tag{A16}$$

$$r_\perp = \frac{\tan^2(\theta_2-\theta_1)}{\tan^2(\theta_2+\theta_1)} \tag{A17}$$

The absorptance of the absorber plate, α, can be calculated by the following empirical correlation.

$$\frac{\alpha}{\alpha_n} = 1-1.5879\times10^{-3}\theta + 2.7314\times10^{-4}\theta^2 - 2.3026\times10^{-5}\theta^3 + 9.0244\times10^{-7}\theta^4 - 1.8\times10^{-8}\theta^5 + 1.7734\times10^{-10}\theta^6 - 6.9937\times10^{-13}\theta^7 \tag{A18}$$

where α_n is the solar absorptance at normal incidence for a flat black surface, which is independent on incident angle.

For a tilted flat-plate solar collector, the absorbed radiation, S, is given based on the total incident radiation I_T and the transmittance-absorptance products

$$S = I_{bH}R_b\overline{\tau\alpha}_b + I_{dH}\left(\frac{1+\cos\beta}{2}\right)\overline{\tau\alpha}_d + I_H\rho_g\left(\frac{1-\cos\beta}{2}\right)\overline{\tau\alpha}_g \tag{A19}$$

where the subscript b, d and g represent beam, diffusion and ground reflection respectively. The beam incident angle is used straightforwardly to determine the value of $\overline{\tau\alpha}_b$; however, effective incident angles should be calculated by the following equations to determine $\overline{\tau\alpha}_d$ and $\overline{\tau\alpha}_g$ for diffusion and ground reflected radiation of a tilted surface.

$$\theta_{ed} = 59.7-0.1388\beta + 0.001497\beta^2 \tag{A20}$$

$$\theta_{eg} = 90-0.5788\beta + 0.002693\beta^2 \tag{A21}$$

The useful thermal energy output from a flat-plate solar collector can be calculated by the following equation.

$$Q_u = A_{sc}F_R[S-U_L(T_i-T_a)] \tag{A22}$$

where A_{sc} is the collector surface area; U_L is the heat loss coefficient; T_i is the inlet HTF temperature; T_a is the ambient temperature; F_R is the collector heat removal factor, which can be estimated based on following equations with the collector dimensions shown in Fig. A4.

$$F_R = \frac{\dot{m}c_p}{A_{sc}U_L}\left[1-\exp\left(-\frac{A_{sc}U_LF'}{\dot{m}c_p}\right)\right] \tag{A23}$$

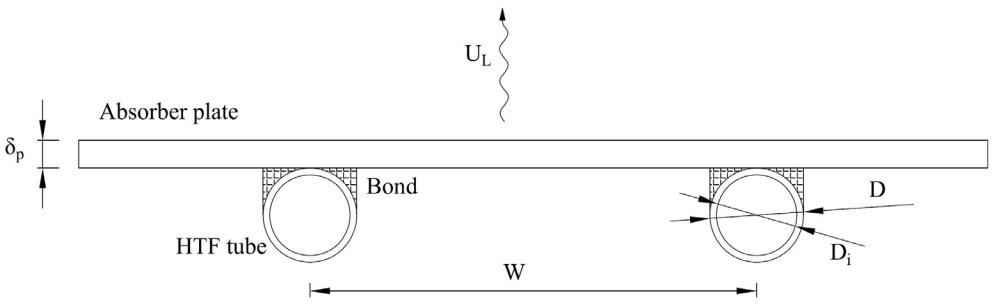

Fig. A4. Sheet and tube in a flat-plate solar collector.

Table A1
Parameters of the used flat-plate collector.[a]

Parameter	Value
K	16 m^{-1}
L	4.2 mm
α_n	0.93
[b]A_{sc}	1.94 m^2
U_L	6 W/(m^2 K)
[c]$\dot{m}$	50 kg/(h m^2)
k	400 W/(m K)
C_b	∞ W/(m K)
W	114 mm
D	10 mm
D_i	8 mm
δ_p	0.5 mm

[a] Based on a real flat-plate collector from SUNSYSTEM®.
[b] Per collector module.
[c] Nominal value.

$$F' = \frac{1/U_L}{W\left[\frac{1}{U_L[D+(W-D)F]} + \frac{1}{C_b} + \frac{1}{\pi D_i h_{fi}}\right]} \tag{A24}$$

$$F = \frac{tanh[m(W-D)/2]}{m(W-D)/2} \tag{A25}$$

$$m = \sqrt{\frac{U_L}{k\delta_p}} \tag{A26}$$

where $\dot{m}$ is the mass flow rate of HTF; c_p is the specific heat of HTF; k is the thermal conductivity of the absorber plate; C_b is the bond conductance; h_{fi} is the HTF heat transfer coefficient, which can be calculated by the classical heat transfer correlations. The parameters of the used flat-plate collector are presented in Table A1.

References

Aydin, D., Casey, S.P., Chen, X., Riffat, S., 2016. Novel 'open-sorption pipe' reactor for solar thermal energy storage. Energy Convers. Manage. 121, 321–334.
Bales, C., 2008. Laboratory tests of chemical reactions and prototype sorption storage units. IEA Task 32.
Department for Business, Energy & Industrial Strategy, 2016. Energy Consumption in the UK.
Duffie, J.A., Beckman, W.A., 2013. Solar Engineering of Thermal Processes, fourth ed. Willey, New Jersey.
Eames, P., Loveday, D., Haines, V., Romanos, P., 2014. The Future Role of Thermal Energy Storage in the UK Energy System: An Assessment of the Technical Feasibility and Factors Influencing Adoption. UKERC.
Energy Saving Trust England. Measurement of domestic hot water consumption in dwellings, 2008. https://www.gov.uk/government/publications/measurement-of-domestic-hot-water-consumption-in-dwellings (Available May 2017).
Finck, C., Henquet, E., van Soest, C., Oversloot, H., de Jong Ard-Jan, Cuypers, R., van't Spijker, 2014. Experimental results of a 3 kWh thermochemical heat storage module for space heating application. Energy Proc. 48, 320–326.
Fisch, M.N., Guigas, M., Dalenback, J.O., 1998. A review of large-scale solar heating system in Europe. Sol. Energy 63, 355–366.
Hadorn, J.C., 2007. Advanced storage concepts for active solar energy IEA-SHC Task 32 2003–2007. In: Proceedings of the First International Congress on Heating, Cooling, and Buildings, Lisbon, Portugal.
Hahne, E., 2000. The ITW solar heating system: an oldtimer fully in action. Sol. Energy 69, 469–493.
Hauer, A., 2002. Thermal energy storage with zeolite for heating and cooling applications. In: Proceedings of 3rd workshop of annex 17 ECES IA/IEA.
Hirano, S., Saitoh, T.S., 2007. Long-term performance of latent heat thermal energy storage using supercooling. In: Proceedings of ISES Solar World Congress 2007: Solar Energy and Human Settlement.
Johnston, D., Siddall, M., 2016. The building fabric thermal performance of passivhaus dwellings-does it do what it says on the tin? Sustainability 8 (1), 97. http://dx.doi.org/10.3390/su8010097.
Johnston, D., Wingfield, J., Miles-Shenton, D., 2010. Measuring the fabric performance of UK dwellings. In: Proceedings of 26th Annual ARCOM Conference, 6–8 September 2010, Leeds, UK.
Kane, T., Firth, S.K., Lomas, K.J., 2015. How are UK homes heated? A city-wide, socio-technical survey and implications for energy modelling. Energy Build. 86, 817–832.
Karacavus, B., Can, A., 2009. Thermal and economical analysis of an underground seasonal storage heating system in Thrace. Energy Build. 41, 1–10.
Mangold, D., Schmidt, T., 2009. The next generations of seasonal thermal energy storage in Germany. ESTEC 2009, Munich, Germany, May 25–26.
Mauran, S., Lahmidi, H., Goetz, V., 2008. Solar heating and cooling by a thermochemical process. First experiments of a prototype storing 60 kWh by a solid/gas reaction. Sol. Energy 82, 623–636.
Michel, B., Mazet, N., Neveu, P., 2014. Experimental investigation of an innovative thermochemical process operating with a hydrate salt and moist air for thermal energy storage of solar energy: global performance. Appl. Energy 129, 177–186.
Palmer, J., Cooper, I., 2013. United Kingdom Housing Energy Fact File. Department of Energy and Climate Change, London.
Pinel, P., Cruickshank, C.A., Beausoleil-Morrison, I., Wills, A., 2011. A review of available methods for seasonal storage of solar thermal energy in residential applications. Renew Sustain Energy Rev 15, 3341–3359.
Stafford, A., Bell, M., Gorse, C., 2012. Building Confidence – A Working Paper. Centre for Low Carbon Futures: York, UK.
Weber, R., Asenbeck, S., Kerskes, H., Druck, H., 2016. SolSpaces-Testing and performance analysis of a segmented sorption store for solar thermal space heating. Energy Proc. 91, 250–258.
Wilson, S., 2010. Dwelling size survey; 2010. < http://webarchive.nationalarchives.gov.uk/20110118095356/http:/www.cabe.org.uk/files/dwelling-size-survey.pdf > . (Available May 2017).
Xu, J., Wang, R.Z., Li, Y., 2014. A review of available technologies for seasonal thermal energy storage. Sol. Energy 103, 610–638.
Zhang, X., Li, M., Shi, W., Wang, B., Li, X., 2014. Experimental investigation on charging and discharging performance of absorption thermal energy storage system. Energy Convers. Manage. 85, 425–434.
Zhao, Y.J., Wang, R.Z., Li, T.X., Nomura, Y., 2016. Investigation of a 10 kWh sorption heat storage device for effective utilization of low-grade thermal energy. Energy 113, 739–747.
Zondag, H., Kikkert, B., Smeding, S., de Boer, R., Bakker, M., 2013. Prototype thermochemical heat storage with open reactor system. Appl. Energy 109, 360–365.